

Uranyl and Strontium Salt Solvation in Room-Temperature Ionic Liquids. A Molecular Dynamics Investigation

Alain Chaumont, Etienne Engler, and Georges Wipff*

Laboratoire MSM, UMR CNRS 7551, Institut de Chimie,
4 rue B. Pascal, 67 000 Strasbourg, France

Received March 14, 2003

Using molecular dynamics simulations, we compare the solvation of uranyl and strontium nitrates and uranyl chlorides in two room-temperature ionic liquids (ILs): [BMI][PF₆] based on 1-butyl-3-methylimidazolium⁺, PF₆⁻ and [EMI]-[TCA] based on 1-ethyl-3-methylimidazolium⁺, AlCl₄⁻. Both dissociated M²⁺, 2NO₃⁻ and associated M(NO₃)₂ states of the salts are considered for the two cations, as well as the UO₂Cl₂ and UO₂Cl₄²⁻ uranyl complexes. In a [BMI]-[PF₆] solution, the “naked” UO₂²⁺ and Sr²⁺ ions are surrounded by 5.8 and 10.1 F atoms, respectively. The first-shell PF₆⁻ anions rotate markedly during the dynamics and are coordinated, on the average, monodentate to UO₂²⁺ and bidentate to Sr²⁺. In an [EMI][TCA] solution, UO₂²⁺ and Sr²⁺ coordinate 5.0 and 7.4 Cl atoms of AlCl₄⁻, respectively, which display more restricted motions. Four Cl atoms sit on a least motion pathway of transfer to uranyl, to form the UO₂Cl₄²⁻ complex. The free NO₃⁻ anions and the UO₂Cl₄²⁻ complex are surrounded by imidazolium⁺ cations (≈4 and 6–9, respectively). The first shell of the M(NO₃)₂ and UO₂Cl₂ neutral complexes is mostly completed by the anionic components of the IL, with different contributions depending on the solvent, the M²⁺ cation, and its counterions. Insights into energy components of solvation are given for the different systems.

Introduction

There is growing interest in room-temperature ionic liquids (ILs) as potential “green” solvents for a broad variety of solutes, ranging from weakly polar to polar ones.^{1–3} ILs have low vapor pressure and are generally composed of an organic cation (e.g., alkylimidazolium derivatives; see Figure 1), while the X⁻ anion can be used to primarily control the water miscibility.⁴ For instance, 1-alkyl-3-methylimidazolium salts of BF₄⁻ are water miscible, PF₆⁻ salts are water immiscible, while AlCl₄⁻ salts are moisture sensitive. With a suitable choice for the X⁻ anion [e.g., PF₆⁻ or N(CF₃SO₂)₂⁻], assisted liquid–liquid extraction of cations can therefore be conducted. Recent examples involve the efficient extraction of alkali and alkaline earth cations from water by crown ethers.^{5–7} Even without ionophoric assistance, some extraction proceeds, due to a cation exchange mechanism, presum-

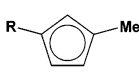
		X ⁻
[BMI][PF ₆]	R= Butyl BMI ⁺	PF ₆ ⁻
[EMI][TCA]	R= Ethyl EMI ⁺	AlCl ₄ ⁻

Figure 1. Ionic components of imidazolium-based ILs.

ably because the X⁻ component of the IL solvates the cation more efficiently than water does.^{7,8} Appending suitable binding groups to the imidazolium cation may lead to “task-specific” ILs, extracting, for example, Hg²⁺ or Cd²⁺ cations.⁹ Recent publications also point to the growing interest in ILs by the nuclear industries (see, for example, ref 10 and references cited therein). So far, very little is known about the microscopic details of the structure of ILs and about their solvation properties, and valuable information emerged from theoretical approaches. Quantum mechanical studies on

* Author to whom correspondence should be addressed. E-mail: wipff@chimie.u-strasbg.fr.

- (1) Seddon, K. R. *J. Chem. Technol. Biotechnol.* **1997**, *68*, 351–356.
- (2) Welton, T. *Chem. Rev.* **1999**, *99*, 2071–2083.
- (3) Wassercheid, P.; Keim, W. *Angew. Chem., Int. Ed.* **2000**, *39*, 3772–3789.
- (4) Hagiwara, R.; Ito, Y. *Fluorine Chem.* **2000**, *105*, 221.
- (5) Dai, S.; Ju, Y. H.; Barnes, C. E. *J. Chem. Soc., Dalton Trans.* **1999**, 1201–1202.
- (6) Visser, A. E.; Swatosli, R. P.; Reichert, W. M.; Griffin, S. T.; Rogers, R. D. *Ind. Eng. Chem. Res.* **2000**, *39*, 3596–3604.
- (7) Dietz, M. L.; Dzielawa, J. A. *Chem. Commun.* **2001**, 2124–2125.

- (8) Chun, S.; Dzyuba, S. V.; Bartsch, R. A. *Anal. Chem.* **2001**, *73*, 3737–3741.
 - (9) Visser, A. E.; Swatosli, R. P.; Reichert, W. M.; Mayton, R.; Sheff, S.; Wierzbicki, A.; Davies, J.; Rogers, R. D. *Environ. Sci. Technol.* **2002**, *36*, 2523–2529.
 - (10) Bradley, A. E.; Hatter, J. E.; Nieuwenhuyzen, M.; Pitner, W. R.; Seddon, K. R.; Thied, R. C. *Inorg. Chem.* **2002**, *41*, 1692–1694.
- Visser, A. E.; Rogers, R. D. *J. Solid State Chem.* **2003**, *171*, 106–113.

selected components of IL provide insights into their conformational or electronic properties,^{11–15} but not sufficient for depicting IL solutions. Molecular dynamics (MD) or Monte Carlo simulations based on empirical representations of the potential energy¹⁶ allow for configurational sampling, and recent reports about the average and dynamic properties of pure ILs,^{17–20} or their solutions with small neutral molecules,²¹ appeared. We therefore decided to investigate by molecular dynamics the solvation of partners involved in the ion extraction to ILs. This paper focuses on two M²⁺ divalent ions, namely, Sr²⁺ and UO₂²⁺, both important in the context of nuclear waste partitioning. Extraction results have been reported for Sr²⁺, which is also a good mimic of the Eu²⁺ cation, recently studied by spectroscopy in an IL.²² In IL solutions, different coordination patterns may be anticipated for Sr²⁺ and UO₂²⁺ because of their different sizes and shapes. In our study, they are formally neutralized by nitrate counterions, also used in extraction experiments to ILs^{5,7,8} and present in concentrated nitric acid solutions of nuclear wastes. As the status of the ion pairs is presently unknown, we consider two initial states where the nitrate salts either are fully dissociated or form intimate ion pairs. They will be noted M²⁺,2NO₃⁻ and M(NO₃)₂, respectively. Given the importance of halide anion coordination to uranyl,²³ we also compare the solvation of the neutral UO₂Cl₂ and negatively charged UO₂Cl₄²⁻ species. The latter is present in chloride-containing ILs,^{24–26} solid-state analogues,^{25,27} and molten melts²⁸ and has been investigated by UV–visible spectroscopy in ILs.²⁶ With regard to the solvent, we consider two ILs, both based on the imidazolium cation, with PF₆⁻ and

AlCl₄⁻ as anions, namely, 1-butyl-3-methylimidazolium⁺,PF₆⁻ ([BMI][PF₆]) and 1-ethyl-3-methylimidazolium⁺,AlCl₄⁻ ([EMI][TCA]). It is indeed interesting to compare the poorly coordinated PF₆⁻ anion with the more coordinating AlCl₄⁻ one and the EMI⁺ cation with the more hydrophobic BMI⁺ one. As a first approach, we assume that all species retain their integrity during the simulation, thus without considering possible reactions such as halide transfer from the IL to the cation or halide elimination to form, for example, Al₂Cl₇⁻ and Cl⁻ species.

Methods

The systems were simulated by classical molecular dynamics (MD) using AMBER 5.0²⁹ in which the potential energy U is described by a sum of bond, angle, and dihedral deformation energies and pairwise additive 1–6–12 (electrostatic and van der Waals) interactions between nonbonded atoms.

$$U = \sum_{\text{bonds}} k_b(b - b_0)^2 + \sum_{\text{angles}} k_\theta(\theta - \theta_0)^2 + \sum_{\text{dihedrals}} \sum_n V_n [1 + \cos(n\varphi - \gamma)] + \sum_{i < j} \left[\frac{q_i q_j}{R_{ij}} - 2\epsilon_{ij} \left(\frac{R_{ij}^*}{R_{ij}} \right)^6 + \epsilon_{ij} \left(\frac{R_{ij}^*}{R_{ij}} \right)^{12} \right]$$

Cross terms in van der Waals interactions were constructed using the Lorentz–Berthelot rules. The parameters used for the ILs have been tested on the pure liquid properties. Those of EMI⁺, BMI⁺, and TCA⁻ ions were taken from Stassen *et al.*,¹⁸ while those of PF₆⁻ were from the OPLS force field³⁰ and have been used by Berne *et al.* to simulate ILs.³¹ The corresponding F parameters have been tested for liquid simulations.³² The parameters for UO₂²⁺,³³ Sr²⁺,³⁴ and NO₃⁻³⁵ were fitted on free energies of hydration. The corresponding AMBER atom types and atomic charges are given in Figure S1 (Supporting Information). The 1–4 van der Waals interactions were scaled down by a factor of 2, and the corresponding Coulombic interactions were scaled down by 1.2, as recommended by Cornell *et al.*³⁶ The solution systems were simulated with three-dimensional periodic boundary conditions. Nonbonded interactions were calculated with a 12 Å atom-based cutoff, correcting for the long-range electrostatics by using the Ewald summation method (PME approximation).^{16,37} Tests on the [EMI]-[TCA] pure liquid using a larger cutoff (15 Å) showed that both cutoffs yield similar results, and the shorter one was thus used to reduce the computational costs.

The MD simulations were performed at 300 K starting with random velocities. The temperature was monitored by coupling the

- (11) Dymek, C. J. J.; Stewart, J. J. P. *Inorg. Chem.* **1989**, *28*, 1472.
- (12) Takahashi, S.; Suzuya, K.; Kohara, S.; Koura, N.; Curtiss, L. A.; Saboungi, M. L. *Z. Phys. Chem.* **1999**, *209*, 209–211.
- (13) Sitze, M. S.; Schreiter, E. R.; Patterson, E. V.; Freeman, R. G. *Inorg. Chem.* **2001**, *40*, 2298–2304.
- (14) Meng, Z.; Dolle, A.; Carper, W. R. *THEOCHEM* **2002**, *585*, 119–128.
- (15) Turner, E. A.; Pye, C. C.; Singer, R. D. *J. Phys. Chem. A* **2003**, *107*, 2277–2288.
- (16) Allen, M. P.; Tildesley, D. J. In *Computer Simulation of Liquids*; van Gunsteren, W. F., Weiner, P. K., Eds.; Clarendon Press: Oxford, U.K., 1987.
- (17) Hanke, C. G.; Price, S. L.; Lynden-Bell, R. M. *Mol. Phys.* **2001**, *99*, 801–809.
- (18) Andrade, J. D.; Böes, E. S.; Stassen, H. *J. Phys. Chem. B* **2002**, *106*, 13344–13351.
- (19) Shah, J. K.; Brennecke, J. F.; Maginn, E. J. *Green Chem.* **2002**, *4*, 112–118.
- (20) Morrow, T. I.; Maginn, E. J. *J. Phys. Chem. B* **2002**, *106*, 12807–12813.
- (21) Hanke, C. G.; Atamas, N. A.; Lynden-Bell, R. M. *Green Chem.* **2002**, *4*, 107–111. Hanke, C. G.; Johansson, A.; Harper, J. B.; Lynden-Bell, R. M. *Chem. Phys. Lett.* **2003**, *374*, 85–90.
- (22) Billard, I.; Moutiers, G.; Labet, A.; ElAzz, A.; Gaillard, C.; Mariet, C.; Lutzenkirchen, K. *Inorg. Chem.* **2003**, *42*, 1726–1733.
- (23) Burns, J. H. In *The Chemistry of the Actinide Elements*, 2nd ed.; Katz, J. L., Seaborg, G. T., Morss, L. R., Eds.; Chapman and Hall: London, 1986; Chapter 20, pp 1417–1479.
- (24) Brittain, H. G.; Perry, D. L.; Tsao, L. *Spectrochim. Acta* **1984**, *40A*, 651–655.
- (25) Zalkin, A.; Perry, D.; Tsao, L.; Zhang, D. *Acta Crystallogr.* **1983**, *C39*, 1186–1188.
- (26) Dai, S.; Shin, Y. S.; Toth, L. M.; Barnes, C. E. *Inorg. Chem.* **1997**, *36*, 4900–4902.
- (27) Perry, D.; Freyberg, D. P.; Zalkin, A. *J. Inorg. Nucl. Chem.* **1980**, *42*, 243–245.
- (28) Dai, S.; Toth, L. M.; DelCul, G. G.; Metcalf, D. H. *J. Phys. Chem.* **1996**, *100*, 220–223.

- (29) Case, D. A.; Pearlman, D. A.; Caldwell, J. C.; Cheatham, T. E., III; Ross, W. S.; Simmerling, C. L.; Darden, T. A.; Merz, K. M.; Stanton, R. V.; Cheng, A. L.; Vincent, J. J.; Crowley, M.; Ferguson, D. M.; Radmer, R. J.; Seibel, G. L.; Singh, U. C.; Weiner, P. K.; Kollman, P. A. *AMBER5*; University of California: San Francisco, 1997.
- (30) Kaminski, G. A.; Jorgensen, W. L. *J. Chem. Soc., Perkin Trans. 2* **1999**, 2365–2375.
- (31) Margulies, C. J.; Stern, H. A.; Berne, B. J. *J. Phys. Chem. B* **2002**, *106*, 12017–12021.
- (32) Gough, C. A.; DeBolt, S. E.; Kollman, P. A. *J. Comput. Chem.* **1992**, *13*, 963–970.
- (33) Guilbaud, P.; Wipff, G. *THEOCHEM* **1996**, *366*, 55–63.
- (34) Åqvist, J. *J. Phys. Chem.* **1990**, *94*, 8021–8024.
- (35) van Veggel, F. C. J. M.; Reinhoudt, D. *Chem. Eur. J.* **1999**, *5*, 90–95.
- (36) Cornell, W. D.; Cieplak, P.; Bayly, C. I.; Gould, I. R.; Merz, K. M.; Ferguson, D. M.; Spellmeyer, D. C.; Fox, T.; Caldwell, J. W.; Kollman, P. A. *J. Am. Chem. Soc.* **1995**, *117*, 5179–5197.
- (37) Essmann, U.; Perera, L.; Berkowitz, M. L. *J. Chem. Phys.* **1995**, *103* (19), 8577–8593.

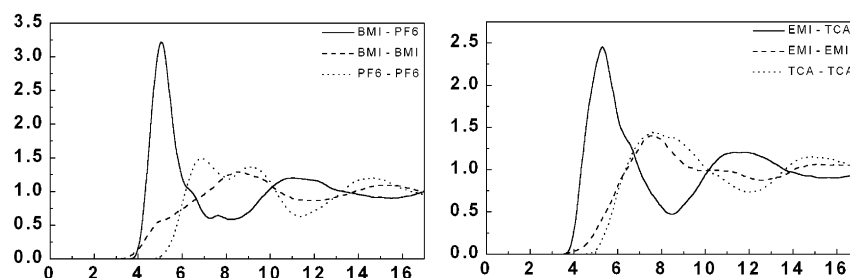


Figure 2. Pure [BMI][PF₆] (left) and [EMI][TCA] liquids (right). Anion–anion, cation–cation, and anion–cation radial distribution functions as a function of the distances (angstroms). Averages over the last 200 ps. Typical snapshots of the first solvation shell of BMI⁺, PF₆[−], EMI⁺, and TCA[−] ions are given in Figure S2.

system to a thermal bath using the Berendsen algorithm with a relaxation time of 0.2 ps. All C–H bonds were constrained with SHAKE, using the Verlet leapfrog algorithm with a time step of 2 fs to integrate the equations of motion.

We first equilibrated “cubic” boxes of pure solvents, containing 150 EMI⁺TCA[−] or 150 BMI⁺PF₆[−] ions, 37.5 and 37.7 Å in length, respectively. This was achieved by repeated sequences of (i) heating the system at 500 K at a constant volume for 0.5 ns followed by (ii) 0.5 ns of dynamics at 300 K and a constant pressure of 1 atm and (iii) 1 ns of dynamics at 300 K and a constant volume. After equilibration, the solvent densities (1.30 and 1.33, respectively) were in fair agreement with experimental values (1.30^{12,38} and 1.36,³⁹ respectively) and the cation–anion radial distribution functions (Figure 2) were similar to those published in refs 18 and 31 and with the neutron diffraction data of the [EMI][TCA] liquid.⁴⁰ Typical snapshots of the first solvation shells are given in Figure S2 (Supporting Information).

We then immersed the solutes in these ILs as M²⁺,2NO₃[−] dissociated ions (distant from ≈13 Å) or as intimate ion pairs for M(NO₃)₂, UO₂Cl₂, and UO₂Cl₄^{2−}. The solvent boxes were 47 Å in length and contained 294 EMI⁺TCA[−] or 294 BMI⁺PF₆[−] ions. The UO₂Cl₄^{2−} solutions were neutralized by removing two solvent anions. Equilibration started with 1500 steps of steepest descent energy minimization, followed by 50 ps of MD with fixed solutes (“BELLY” option of AMBER) at a constant volume and by 25 ps at a constant volume without constraints, followed by 25 ps at a constant pressure of 1 atm. The subsequent MD trajectories of 1.2 ns were saved every 0.5 ps and analyzed with the MDS and DRAW software.⁴¹ For each dissociated ion pair, two independent simulations were performed to check that the sampling was sufficient and that the final solvation patterns were the same. In the case of UO₂²⁺, another sampling test involved randomization of the system at 500 K for 0.5 ns using biased potentials (with all Coulombic interactions divided by 100), followed by 1 ns of dynamics at 300 K with the original potentials. Insights into the energy component were obtained by group analysis, using a 17 Å cutoff distance and a reaction field correction for the electrostatics.⁴²

The average structure of the solvent was characterized by the radial distribution functions (RDFs) of the Al, Cl, P, and F atoms of the anions and of the N_{ethyl} (EMI⁺) or N_{butyl} (BMI⁺) atoms of imidazolium cations of the solvents around the U_{UO₂}, Sr, and N_{NO₃} atoms of the solutes during the last 0.2 ns.

Results

We first describe the structural characteristics of the solvation of the “naked” ions and their “complexes” with nitrate and chloride anions in the two solvents (sections 1–3). This is followed by an energy analysis of their solvation.

1. M²⁺,2NO₃[−] Dissociated Ion Pairs in [BMI][PF₆] versus [EMI][TCA] Solutions. The solvent RDFs (Figure 3 and Table 1) and typical snapshots of first-shell solvent molecules (Figures 4 and S6) show that the ionic components of the ILs specifically solvate the M²⁺ and NO₃[−] ions. In both liquids, the cations are fully surrounded by X[−] anions of the solvent, with marked differences, depending on the nature of M²⁺ and X[−].

We first consider the uranyl cation in a [BMI][PF₆] solution. The U atom is surrounded, on average, by 6.0 ± 0.1 PF₆[−] anions. The U–P RDF displays a narrow peak, indicating that the six P atoms are quasi-equidistant from U (4.0 Å). They form an arrangement of approximate D₃ symmetry with three P atoms above and three P atoms below the equatorial plane of UO₂²⁺. The two triplet O–U–P angles (≈112° and 65 ± 5°; see Figure S3) oscillate but do not exchange during the dynamics, as also seen from the sharp peak of the RDF and the very small fluctuation in the U–(P) coordination number. See also the time evolution of the shortest U–P distances (Figure S5). With regard to the corresponding F atoms, the situation is somewhat more complex. A first peak at 2.6 Å integrating to 5.8 ± 0.6 F atoms is followed by a broader region up to 6.5 Å corresponding to the “nonbonded” F atoms. Visual inspection of the trajectories shows that the anions rotate during the dynamics, exchanging their “coordinated” F atoms.⁴³ During the last 0.5 ns of dynamics, all 6 × 6 F atoms contributed to the first peak, and PF₆[−] anions exchanged between monodentate and bidentate coordination to the U atom. The RDF of BMI⁺ becomes non-zero after 6 Å and integrates to 4.9 ± 1.1 cations up to 7.5 Å. A typical view (Figure 4) shows that one of them solvates axially the O uranyl atom on one side, while three others cap the three PF₆[−] anions on the other side.

The solvation of Sr²⁺ in the same solvent is easier to describe, as Sr²⁺ is surrounded by a cage of 5 PF₆[−] anions,

(38) Fannin, A. A.; Floreani, D. A.; King, L. A.; Landers, J. S.; Piersma, B. J.; Stech, D. J.; Vaughn, R. L.; Wilkes, J. S.; Williams, J. L. *J. Phys. Chem.* **1984**, *88*, 2614.

(39) Gu, Z.; Brennecke, J. F. *J. Chem. Eng. Data* **2002**, *47*, 339.

(40) Takahashi, S.; Suzuka, K.; Kohara, S.; Koura, N.; Curtiss, L. A.; Saboungi, M. L. *Z. Phys. Chem.* **1999**, *209*, 209.

(41) Engler, E.; Wipff, G. Unpublished results.

(42) Tironi, I. G.; Sperb, R.; Smith, P. E.; van Gunsteren, W. F. *J. Chem. Phys.* **1995**, *102*, 5451–5459.

(43) An illustration can be seen in Figure S3 where the U–F distances are plotted during the last 0.1 ns of the simulation, selecting those F atoms which come within 3.4 Å of the U atom, and therefore contribute to the first peak of the RDF during that period, i.e., 11 F atoms. One observes exchanges between the coordinated F atoms (at 2.5 Å) and more remote ones (at 3.5 and 4.5 Å).

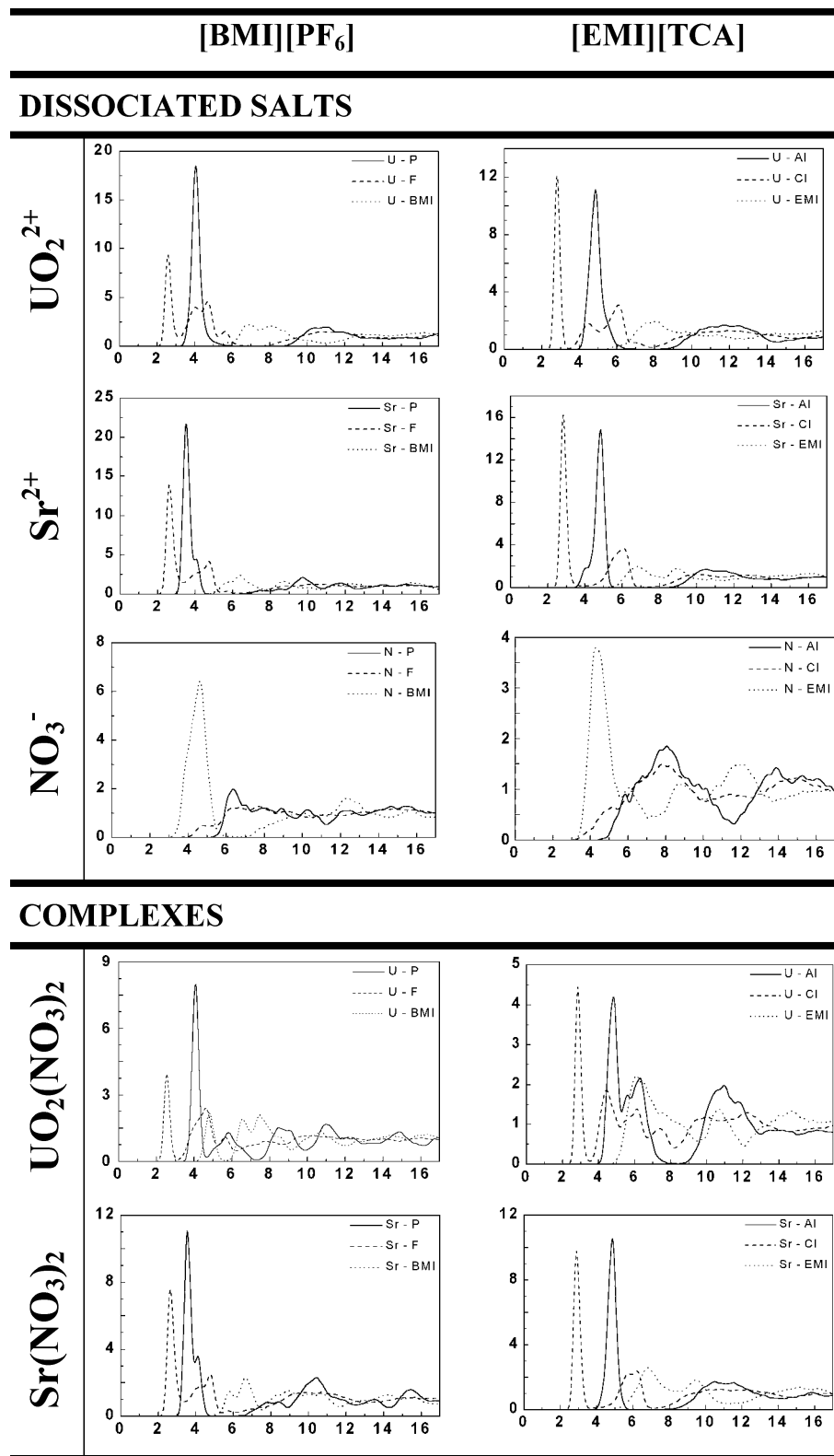


Figure 3. UO_2^{2+} , 2NO_3^- and Sr^{2+} , 2NO_3^- salts (dissociated *versus* intimate ion pairs) in IL solutions. Radial distribution functions of the liquid around the U, Sr, and N_{NO_3} atoms. Distances are in angstroms.

leading to a clear first peak in the RDF with 5.0 ± 0.1 P atoms and 10.1 ± 0.9 F atoms, i.e., in a 1:2 ratio. The anion cage is of C_4 -type symmetry, with 4 basal Sr–P distances of 3.4 Å and a longer apical one at 4.1 Å. The anions are generally bidentate, but undergo important rotational motions, leading to transient combinations such as one tridentate, one

monodentate, and three bidentate anions. The importance of dynamics can be seen from the number of different F atoms that visit the Sr^{2+} coordination, i.e., 24 F atoms during the last 0.1 ns and all 6×5 F atoms during 0.25 ns. Exchanges are thus somewhat faster around Sr^{2+} than around UO_2^{2+} , presumably because of “gearing”-type interactions between

Table 1. Uranyl and Strontium Salts in IL Solutions^a

	[BMI][PF ₆]			[EMI][TCA]		
	P	F	BMI	Al	Cl	EMI
Dissociated salts						
UO ₂ ²⁺	6.0 ± 0.1 (4.05; 6.5)	5.8 ± 0.6 (2.6; 3.2)	4.1 ± 0.8 (b; 7.5)	7.0 ± 0.0 (4.85; 7.3)	5.0 ± 0.1 (2.8; 3.45)	4.9 ± 1.1 (b; 8)
Sr ²⁺	5.0 ± 0.1 (3.5; 4.6)	10.1 ± 0.9 (2.6; 3.3)	4.7 ± 0.9 (6.35; 7.9)	7.0 ± 0.0 (4.85; 5.7)	7.4 ± 0.5 (2.85; 3.9)	5.7 ± 0.9 (6.85; 8.3)
NO ₃ ⁻	4.1 ± 0.8 (b; 7.5)	23.3 ± 2.3 (b; 7.5)	5.0 ± 0.1 (4.6; 6.6)	5.3 ± 1.1 (b; 8)	22.2 ± 2 (b; 8)	4.3 ± 0.8 (4.25; 5.6)
Complexes						
UO ₂ (NO ₃) ₂	1.6 ± 0.5 (4.1; 4.6)	2.0 ± 0.2 (2.55; 3.15)	1.0 ± 0.1 (4.8; 5.7)	2.7 ± 0.6 (4.7; 5.9)	2.0 ± 0.1 (2.9; 3.45)	0.6 ± 0.5 (5.2; 5.9)
UO ₂ Cl ₂	2.3 ± 0.5 (4.1; 4.9)	2.7 ± 0.6 (2.6; 3.2)	3.7 ± 1.1 (6.3; 7.4)	2.8 ± 0.6 (4.9; 5.5)	2.9 ± 0.6 (2.8; 4.0)	10.5 ± 0.9 (6.5; 9.5)
UO ₂ Cl ₄ ²⁻	2.0 ± 0.6 (6.9; 7.5)	2.6 ± 1.1 (5.3; 6.0)	6.1 ± 0.6 (5.8; 7.5)	2.3 ± 0.7 (6.9; 7.7)	2.1 ± 0.9 (5.0; 6.0)	8.6 ± 0.7 (5.7; 7.8)
Sr(NO ₃) ₂	3.0 ± 0.0 (3.55; 4.8)	5.8 ± 0.6 (2.65; 3.4)	4.3 ± 0.5 (6.65; 7.6)	4.8 ± 0.4 (4.8; 5.85)	4.8 ± 0.4 (2.85; 3.9)	8.9 ± 0.7 (6.8; 8.75)

^a Characteristics of the first peak of the radial distribution function around the U, Sr, and N_{NO₃} atoms: coordination number and fluctuations and, in parentheses, distances (in angstroms) of the first maximum and minimum. Values are averages over the last 0.6 ns of MD. ^b Value not reported because there is no clear maximum.

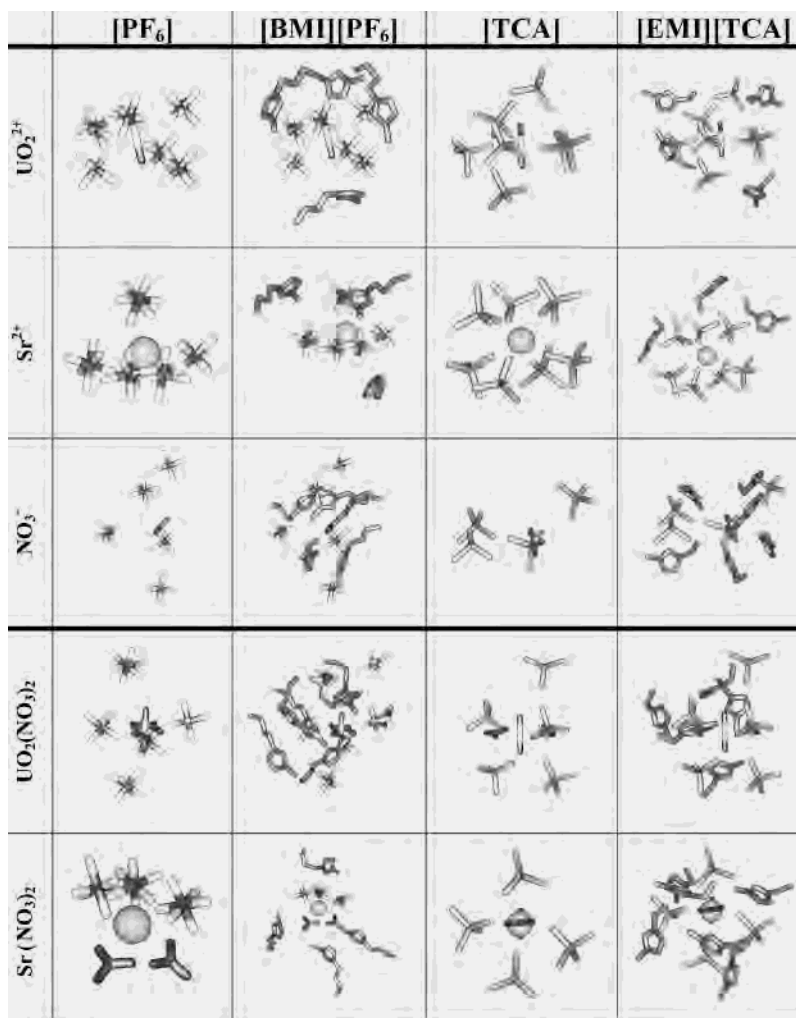


Figure 4. UO₂²⁺, 2NO₃⁻ and Sr²⁺, 2NO₃⁻ salts (dissociated *versus* intimate ion pairs) in [BMI][PF₆] and [EMI][TCA] solutions. Snapshot of the first solvation shell of uranyl, strontium, and nitrate after 1.2 ns. The time evolution of the shortest M–P, M–Al, M–F, and M–Cl distances (M is U or Sr) is given in Figures S4 and S5. A color version of this figure appears as Figure S6.

the PF₆⁻ anions in the more symmetrical environment. The Sr–BMI⁺ cation RDF starts at 6.5 Å, and from there to the first minimum (at ≈7.9 Å), one finds 4.7 ± 0.9 cations which therefore sit in the second shell.

With regard to the NO₃⁻ anions, their solvation is found to be the same for the two salts, in relation to their large separation (12–17 Å) from the M²⁺ cations. A first well-defined peak in the RDF at 4.6 Å corresponds to 5.0 ± 0.1

BMI⁺ cations, which form a quite rigid cage around NO₃⁻ (see Figure 4). Note the small fluctuations, which contrast with the large ones observed around the M²⁺ ions.

We now consider the [EMI][TCA] solvent which also displays specific interactions with the dissociated ions. The U–AlCl₄⁻ RDF displays two well-defined peaks (Figure 3) corresponding to 5.0 ± 0.1 Cl atoms at 2.8 Å and to 7.0 ± 0.0 Al atoms at 4.85 Å. The very small fluctuations contrast with the large ones observed with PF₆⁻ anions, indicating a fairly rigid coordination.⁴⁴ Very interestingly, visual inspection of the trajectories shows that the four “equatorial” Cl atoms form the shortest bonds with the U atom, therefore sitting on the least motion pathway of transfer to uranyl, leading to the UO₂Cl₄²⁻ species. The first-shell AlCl₄⁻ anions shield UO₂²⁺ from the EMI⁺ cations, five of which sit, on average, in an ill-defined second shell (up to 8 Å).

The first solvation shell of Sr²⁺ is again simpler, and consists of 7.0 ± 0.0 AlCl₄⁻ anions with a contribution of 7.4 ± 0.5 Cl atoms at 3.9 Å. Thus, the anions display most often monodentate coordination to Sr²⁺ but are sometimes bidentate. With regard to the NO₃⁻ anions, they are surrounded by a cage of 4.3 EMI⁺ cations, which shield them from the solvent anions.

2. M(NO₃)₂ Intimate Ion Pairs in [BMI][PF₆] versus [EMI][TCA] Solutions. During the dynamics, the UO₂(NO₃)₂ and Sr(NO₃)₂ salts were free of constraints, but remained associated, generally with bidentate nitrates. In the two liquids, the two nitrates, which were initially *trans*, retained this *trans* relationship in the equatorial plane of UO₂²⁺, but for Sr²⁺, their coordination mode was solvent-dependent. In [BMI][PF₆], they became *cis*, while in [EMI][TCA], they preferred a least repulsion *D_{2d}*-type arrangement. In all cases, the M²⁺ cations are partly shielded from the IL. Analysis of the RDFs (Figure 3) is reported in Table 1 and illustrated by typical snapshots at the end of the simulation (Figure 4). Although the salts are formally neutral, their first solvation shell is completed by solvent anions, which do not exchange with the “bulk” ones.

In a [BMI][PF₆] solution, the U atom of UO₂(NO₃)₂ coordinates 2.0 ± 0.2 F atoms at 2.5 Å in its equatorial plane, which dynamically exchange with F atoms at ≈4.6 Å, corresponding to an average of 1.6 ± 0.5 PF₆⁻ anions only. Note that the exchange (~1 every 20 ps) is slower than around the naked cation (by a factor of 2–3) and that the PF₆⁻ anions, most often monodentate, also achieve transient bidentate coordination.

The first shell of Sr(NO₃)₂ is similarly completed by F atoms, 5.8 ± 0.6 on average, corresponding to 3.0 ± 0.0 PF₆⁻ anions which are in majority bidentate. This may explain why the nitrates remain “*cis*”. The strontium and

uranyl salts are also in direct contact with an average of ≈4.0 BMI⁺ cations via their nitrate and O_{UO₂} oxygens. These BMI⁺ cations are, however, farther (at ~5 Å) from the Sr or U atoms than are the first-shell X⁻ anions.

In an [EMI][TCA] solution, the anions also determine the first solvation shell of the nitrate salts. The U atom of UO₂(NO₃)₂ coordinates an average of 2.0 ± 0.1 Cl atoms at 2.9 Å near its equatorial plane, which sometimes exchange with the other Cl atoms of the corresponding (2.7, on average) AlCl₄⁻ anions. The exchange is more limited than with PF₆⁻ anions and synchronized with transient changes from bidentate to monodentate nitrate coordination. The first coordination shell of the Sr atom of Sr(NO₃)₂ is similarly completed by 4.8 Cl atoms, corresponding to 4.8 AlCl₄⁻ ions which oscillate between monodentate (in majority) and bidentate coordination, with nonlinear Sr–Cl–Al angles (see Figure 4). With regard to the “first-shell” EMI⁺ cations, they are farther than the anions from the two solutes (at ~5 Å), especially in the case of Sr(NO₃)₂, where Sr is best shielded by the coordinated NO₃⁻ and AlCl₄⁻ anions.

3. UO₂Cl₂ and UO₂Cl₄²⁻ Intimate Ion Pairs in [BMI][PF₆] versus [EMI][TCA] Solutions. In the two solvents, the UO₂Cl₂ and UO₂Cl₄²⁻ species remained bound, with U–Cl distances (≈2.56 Å on average) in fair agreement with the value of 2.67 Å observed in the X-ray structure of UO₂Cl₄(imidazolium)₂.²⁵ Solvent RDFs are shown in Figure 5, and their characteristics are summarized in Table 1. Typical snapshots are shown in Figures 6 and S8.

In both solvents, the first shell of UO₂Cl₂ is completed by solvent anions, as for the UO₂(NO₃)₂ salt, with somewhat different CNs, though. In a [BMI][PF₆] solution, one finds 2.7 ± 0.6 coordinated F atoms, stemming from 2.3 PF₆⁻ anions, on average, leading to an equatorial total CN of 4.7 halides. One PF₆⁻ is generally monodentate, while another is more mobile and often bidentate. Similarly, in an [EMI][TCA] solution, the first uranyl shell is completed by 2.9 ± 0.6 Cl atoms of 2.8 ± 0.6 AlCl₄⁻ anions which are mostly monodentate. Notice the high fluctuations, indicative of the dynamics coordination, and the somewhat larger CNs, as compared to those of UO₂(NO₃)₂, in keeping with the smaller equatorial steric demand of chloride, compared to nitrate ions. Imidazolium cations are more remote than the solvent anions: their RDFs start being non-zero at ≈6 Å in the two liquids (Figure 5).

The solvation of UO₂Cl₄²⁻ is characterized by a marked imidazolium peak in both solvents, somewhat broader in a [BMI][PF₆] than in an [EMI][TCA] solution. Integration up to the first minimum (at ≈7.8 Å) gives 6.1 ± 0.6 BMI⁺ and 8.6 ± 0.7 EMI⁺ cations. One also finds solvent anions at these distances, 2.0 PF₆⁻ and 2.3 AlCl₄⁻ anions on average. Interestingly, in both solvents, two anions sit close to an “axial” position with respect to uranyl (Figure 6), and in an [EMI][TCA] solution, another AlCl₄⁻ anion is more “equatorial”. With regard to the BMI⁺ or EMI⁺ cations, they adopt all kinds of dynamically exchanging positions and orientations around UO₂Cl₄²⁻, as illustrated in Figure 6. Some of them contact the anionic solute via their aromatic rings, in a tangential or perpendicular fashion. Others rather point an

(44) This is confirmed by the time evolution of the U–Cl distances, again selecting those Cl atoms which contribute to this first peak of the U–Cl RDF (i.e., which sit within 3.5 Å of U) during the last 0.1 ns. It can be seen in Figure S4 that only five Cl atoms are involved in the equatorial coordination and thus do not exchange with the 23 others of the seven first-shell AlCl₄⁻ anions. Among these, two are in fact close to apical positions (<O–U–Al angles are 137 and 34°), four are close to the equatorial plane (<O–U–Al angles are 76–88°), and one is intermediate (<O–U–Al angle = 117°; see Figure S3).

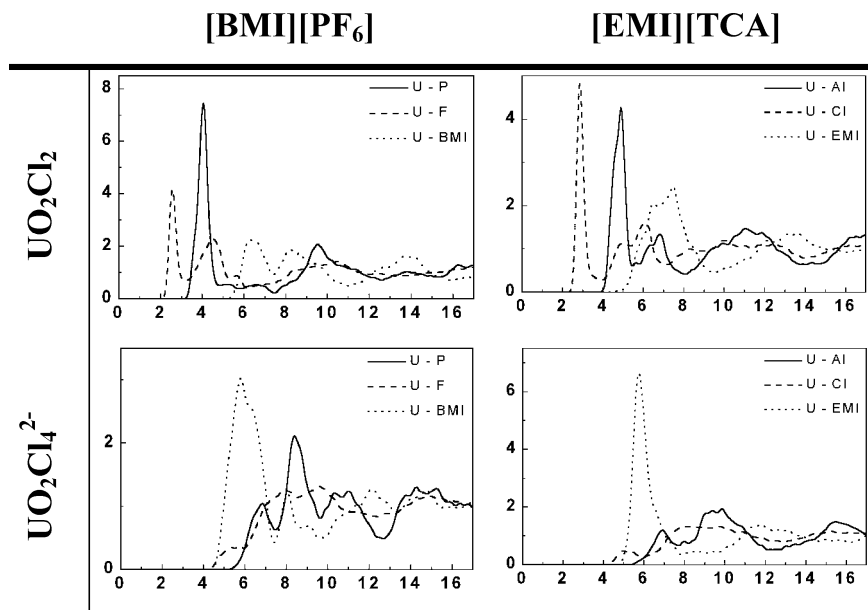


Figure 5. UO_2Cl_2 and $\text{UO}_2\text{Cl}_4^{2-}$ complexes in IL solutions. Radial distribution functions of the liquid around the U atom. Distances are in angstroms.

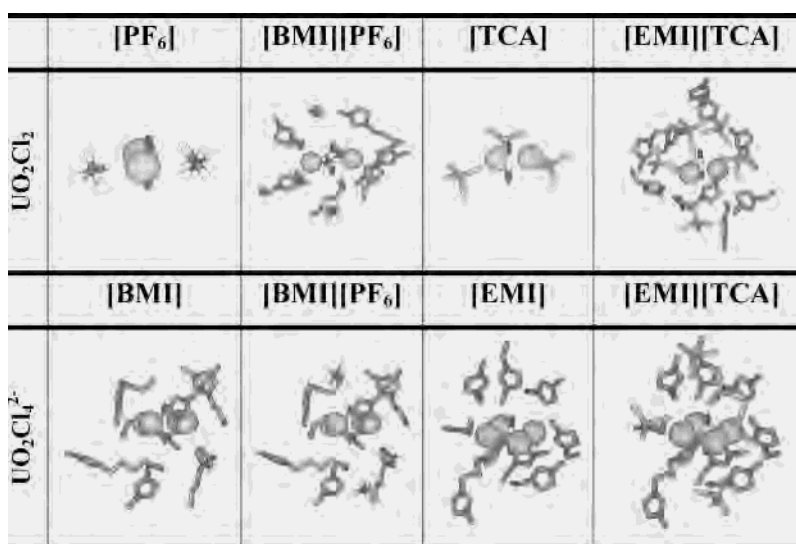


Figure 6. UO_2Cl_2 and $\text{UO}_2\text{Cl}_4^{2-}$ complexes in IL solutions. Snapshot of the first solvation shell after 1.2 ns. The time evolution of the shortest U–P, U–Al, U–F, and U–Cl distances is given in Figures S7. A color version of this figure appears as Figure S8.

alkyl chain. These patterns result from the interplay between solvent–solvent and solute–solvent interactions and dramatically differ from those observed, for example, in the solid-state structure of the $\text{UO}_2\text{Cl}_4(\text{imidazolium})_2$ salt which consists of columns of $\text{UO}_2\text{Cl}_4^{2-}$ anions and columns of $\text{CH}_3\text{C}_3\text{N}_2\text{H}_4^+$ cations.²⁵

4. Insights into Energy Features of Solvation. As a result of specific solvation, the energies of the interaction between the solute and solvents depend on the shape and size of the M^{2+} cation, on the status of its counterions, and on the solvent. In this section, we discuss average solvent solute interaction energies ΔE 's, derived from an energy component analysis in terms of the contributions of the different species. The main results are given in Tables 2 and S1.

All ΔE 's all negative (from approximately -100 kcal/mol for neutral complexes to approximately -460 kcal/mol for naked M^{2+} cations) and larger in magnitude than the energy of the interaction between a single solvent ion and the

rest of the solvent (from -80 to -100 kcal/mol), indicating stabilizing interactions between the solutes and the ILs. Dissection of ΔE into the XMI^+ and Y^- contributions of the solvents (noted ΔE^+ and ΔE^- , respectively) confirms the solvation features described above. For the naked M^{2+} cations, ΔE^+ is repulsive and smaller in magnitude than ΔE^- which is attractive, while the reverse holds for NO_3^- and the negatively charged $\text{UO}_2\text{Cl}_4^{2-}$ complex. For the neutral $\text{M}(\text{NO}_3)_2$ and UO_2Cl_2 complexes, both contributions are attractive.

With regard to the naked cations, UO_2^{2+} interacts better than Sr^{2+} with [BMI][PF₆] (by ≈ 30 kcal/mol, mostly due to weaker repulsions with the BMI⁺ cations), while Sr^{2+} interacts better with the [EMI][TCA] solvent (by ≈ 10 kcal/mol, mostly due to better interactions with TCA⁻ anions). Comparing now a given cation in the two ILs, one sees that UO_2^{2+} “prefers” [BMI][PF₆] over [EMI][TCA] (by ≈ 35 kcal/mol, mostly because of its stronger interactions with PF₆⁻),

Table 2. Average Interaction Energies ΔE and Fluctuations (kilocalories per mole) between the Solute and the Solvent of Uranyl and Strontium Salts in IL Solutions^a

	[BMI][PF ₆]			[EMI][TCA]		
	ΔE^+	ΔE^-	ΔE	ΔE^+	ΔE^-	ΔE
Pure liquids						
XMI ⁺	457 ± 8	-556 ± 8	-99 ± 7	483 ± 6	-576 ± 6	-93 ± 6
Y ⁻	-563 ± 7	483 ± 8	-81 ± 6	-577 ± 7	485 ± 6	-92 ± 6
Dissociated salts						
UO ₂ ²⁺	930 ± 13	-1390 ± 15	-461 ± 13	923 ± 15	-1348 ± 17	-425 ± 12
Sr ²⁺	991 ± 14	-1419 ± 15	-429 ± 11	942 ± 15	-1374 ± 17	-432 ± 13
2NO ₃ ⁻	-1157 ± 13	933 ± 10	-224 ± 9	-1218 ± 12	989 ± 10	-229 ± 10
Complexes						
UO ₂ (NO ₃) ₂	-72 ± 4	-35 ± 5	-106 ± 6	-71 ± 4	-45 ± 6	-117 ± 8
UO ₂ Cl ₂	-46 ± 4	-50 ± 5	-96 ± 6	-71 ± 7	-66 ± 9	-137 ± 13
UO ₂ Cl ₄ ²⁻	-1139 ± 4	861 ± 6	-278 ± 5	-1196 ± 14	904 ± 14	-292 ± 12
Sr(NO ₃) ₂	-50 ± 5	-119 ± 7	-169 ± 8	-67 ± 4	-97 ± 7	-163 ± 9

^a ΔE^+ corresponds to XMI⁺ (BMI⁺ or EMI⁺) and ΔE^- to Y⁻ (PF₆⁻ or TCA⁻). More details are given in Table S1.

while Sr²⁺ has no marked solvent preference. These results thus suggest possible sources of monitoring the extraction selectivity or solubility of linear *versus* spherical ions by adequate choice of an IL anion.

With regard to neutral nitrate complexes, Sr(NO₃)₂ interacts better than UO₂(NO₃)₂ with the two liquids, and the largest difference (≈ 60 kcal/mol) is found in [BMI][PF₆]. The strontium salt interacts more with the TCA⁻ or PF₆⁻ anions than with the imidazolium cations, while uranyl nitrate interacts better with the imidazolium cations. Comparing now a given salt in the two solvents yields smaller discriminations: UO₂(NO₃)₂ prefers [EMI][TCA] over [BMI][PF₆] by ≈ 10 kcal/mol, while Sr(NO₃)₂ prefers [BMI][PF₆] by ≈ 5 kcal/mol. The role of the complexed anion can be seen in UO₂-Cl₂ *versus* UO₂(NO₃)₂, and the results are found to be solvent-dependent. In contrast to the nitrate salt, the chloride salt interacts better with [EMI][TCA]. With regard to the naked nitrate anion, it also interacts ≈ 40 kcal/mol better with [EMI][TCA], due to differences in ΔE^+ and ΔE^- contributions of the solvent ions (Table 2). UO₂Cl₄²⁻ also prefers the [EMI][TCA] solvent (by ≈ 15 kcal/mol), and this is mainly due to stronger ΔE^+ interactions with imidazolium⁺ cations.

Discussion and Conclusion

We present the first simulation study on Sr²⁺ and UO₂²⁺ ion solvation in two ILs, comparing the naked cations and their nitrate or chloride salts, forming intimate ion pairs. This is based on classical molecular dynamics, using a 1-6-12 potential for the nonbonded interactions, and an important issue is the reliability and quality of this potential. Due to the lack of experimental data for the thermodynamic and structural aspects of ion solvation in ILs, there is presently no way to directly compare the predicted results with experiment. It is thus important to validate the approach *per se*, and there are indeed a number of important positive results obtained on the hydration on these ions. The parameters used for Sr²⁺ and UO₂²⁺ are not standard but have been fitted on free energies of solvation (hydration), which represent the most important thermodynamic quantity. According to the calculations, Sr²⁺ is better hydrated than UO₂²⁺ (by 14.6 ± 3 kcal/mol), in excellent agreement with the experimental value of 13.6 kcal/mol.³³ As discussed in refs 33 and 34, the M²⁺ cation parameters also nicely

reproduce the corresponding hydration numbers of 8-9 and 5, respectively, together with the correct M-O distances in solution. The force field also correctly predicts the binding selectivities of different receptors (e.g., an uranophile calix[6]arene⁶⁻ prefers UO₂²⁺³³ while another amide-substituted calix[4]arene prefers Sr²⁺⁴⁵). This uranyl model has also been used to simulate quartz-water interfaces.⁴⁶ We note that a similar parameter fitting procedure has been used to develop 1-6-12 parameters for trivalent lanthanide cations, also leading to correct calculated absolute and relative hydration energies and to correct binding selectivities by a crown ether in a nonaqueous solvent.^{35,47} This does not mean that many-body, charge transfer, and polarization effects are not important.⁵⁴ Most of them are in fact implicitly incorporated via biased pairwise additive potentials. The latter thus do not aim to reproduce, for example, the interaction between an ion and a single *S* (or a few) solvent molecule(s), as investigated by QM methods.⁵⁵⁻⁵⁷ Conversely, potentials derived by retrodissection of interaction energies in gas-phase Mⁿ⁺...*S* adducts, although accounting in principle

- (45) Muzet, N.; Wipff, G.; Casnati, A.; Domiano, L.; Ungaro, R.; Ugozzoli, F. *J. Chem. Soc., Perkin Trans. 2* **1996**, 1065.
- (46) Greathouse, J. A.; O'Brien, R. J.; Bemis, G.; Pabalan, R. T. *J. Phys. Chem. B* **2002**, *106*, 1646-1655.
- (47) Similarly developed 1-6-12 parameters for halide anions account for their hydration properties and their recognition by synthetic hosts in solution.⁴⁸ Efficient 1-6-12 solvent parameters have also been fitted for pure liquids,⁴⁹ and these have been used later to gain important insights into the solvation of all kinds of solutes,⁵⁰⁻⁵² involving charged heterogeneous systems (e.g., protein-ligand recognition in solution⁵³).
- (48) McDonald, N. A.; Duffy, E. M.; Jorgensen, W. L. *J. Am. Chem. Soc.* **1998**, *120*, 5104-5111.
- (49) Jorgensen, W. L.; Briggs, J. M.; Contreras, M. L. *J. Phys. Chem.* **1990**, *94*, 1683-1686.
- (50) Hummer, G.; Garbe, S.; Garcia, A. E.; Pratt, L. R. *Chem. Phys.* **2000**, *258*, 349-370.
- (51) Guillot, B.; Guissani, Y.; Bratos, S. *J. Chem. Phys.* **1991**, *95*, 3643-3648.
- (52) Åqvist, J.; Warshel, A. *J. Am. Chem. Soc.* **1990**, *112*, 2860-2868.
- (53) Simonson, T.; Archontis, G.; Karplus, M. *Acc. Chem. Res.* **2002**, *35*, 430-437.
- (54) We note, however, that the effects of charge transfer and polarization on solvation properties are less important for neutral M(NO₃)₂ and UO₂Cl₂ complexes or for charged UO₂Cl₄²⁻ complexes than in the case of naked M²⁺ ions whose presence in the studied ILs remains hypothetical.
- (55) Kollman, P. *J. Am. Chem. Soc.* **1977**, *99*, 4875.
- (56) Hemmingsen, L.; Amara, P.; Ansoborlo, E.; Field, M. *J. Phys. Chem. A* **2000**, *104*, 4095.
- (57) Clavaguera-Sarrio, C.; Brenner, V.; Hoyau, S.; Marsden, C. J.; Millié, P.; Dognon, J.-P. *J. Phys. Chem. B* **2003**, *107*, 3051-3060.

for electronic reorganization effects, have not been proven so far to be able to reproduce the free energy of solvation of M^{n+} in the S solution, or solvation in heterogeneous mixtures.⁵⁸ Each approach has its merits and limitations. Promising perspectives emerge from CP-MD simulations which in principle account for electronic reorganization and dynamic effects.⁵⁹ They are, however, presently limited by the representation of f elements and by the short time scales (≈ 10 ps) which are insufficient for performing important configuration sampling. In the studied IL solutions, the interactions are mainly electrostatic in nature, and our simulations properly account for these. An important feature concerns the atomic charge distribution of the liquid ions, and it is worth noting that the ones we used were derived from high-quality QM-calculated electrostatic potentials on imidazolium derivatives and on the anions, and should therefore account for the stereochemistry of the related interactions.^{55,60} According to the studies performed by others^{17,18,20,31} and ourselves, the models account for the main properties of the pure ILs whose structure is mainly determined by “cation–anion coulombic interactions with local steric effects influencing the final orientation”.⁶¹ A further validation comes from a comparison we performed on QM (HF level with a 6-31G** basis set with BSSE-corrected interaction energies) versus AMBER optimizations on the $BMI^+PF_6^-$ dimer. With both methods, the structures are similar while the interaction energies (-76.2 and -75.9 kcal/mol, respectively) are in excellent agreement. Thus, although there is no doubt room for further improvements, we believe that our simulation results, based on accurately fitted parameters, are at least reasonable.

Not surprisingly, we find that the anionic X^- component of the studied ILs dominantly contributes to the first solvation shell of the strontium and uranyl cations, be they naked or forming neutral nitrate or chloride complexes. The simulations reveal specific solvation patterns as a function of the shape of the M^{2+} cation and of the nature of X^- . These are dynamic in nature, and thus static models could hardly account for them. The imidazolium counterpart sits in the second solvation shell of the M^{2+} cations, or contributes weakly to the first shell of the $M(NO_3)_2$ and UO_2Cl_2 salts, but efficiently solvates the naked NO_3^- anions as well as the $UO_2Cl_4^{2-}$ complex. In contrast to simulation results in diluted aqueous solutions, where the nitrate salts dissociate, the latter retain here their imposed starting relationship. Diffusion is much slower in ILs than in traditional solvents, but is fast enough to rapidly (generally less than 10 ps) solvate the studied solutes, without exchanging later with other solvent molecules. Although interactions in ILs are

dominated by electrostatics,⁶¹ it is important to note that the first solvation shell does result not only from solvent–solute interactions but also from solvent–solvent interactions, possibly leading to different coordination numbers in the IL than in the gas phase.⁶² To our knowledge, there is presently no experimental comparison of the simulated solutions. The results, however, hint at the potential of ion separation by ILs with promising applications in the field of ion partitioning. It is also stressed that solvent impurities (e.g., traces of water) or co-ions (e.g., Cl^- in an [EMI][TCA] solution) may strongly compete with the solvent to solvate the ionic solutes, as well as to possibly change their nature (via formation of, for example, $UO_2Cl_4^{2-}$ or $SrCl_n^{2-n}$ species). A recent study indeed pointed to the importance of solvent impurities in the spectroscopic properties and solubility of ions in ILs.²² The nature of the salts has to be studied experimentally (e.g., spectroscopic and diffraction methods) and represents a challenge for future computations (using, for example, potential of mean force calculations).⁶⁵ With regard to uranyl, there is so far, to our knowledge, no characterization of the naked cation in the studied neat ILs, while the $UO_2Cl_4^{2-}$ adduct is commonly observed in chloride-containing ILs,^{24,26,66} as in the X-ray structure of corresponding imidazolium salts.^{25,27} As shown by our simulations in an [EMI][TCA] solution, $UO_2Cl_4^{2-}$ can easily form via a chloride least motion transfer from $AlCl_4^-$. While computer computations alone can hardly predict the ion solubility as a function of counterions, they certainly provide important microscopic insights into the solvation patterns of selected model species in well-defined environments. What happens with other solvent anions [e.g., $N(SO_2CF_3)_2^-$] with which uranyl has been studied,⁶⁷ or mixed solvent components (e.g., $AlCl_4^-$, $AlCl_3$, Cl^- , and $Al_2Cl_7^-$), is beyond the scope of this paper and deserves further investigation.

Acknowledgment. We are grateful to IDRIS, CINES, Université Louis Pasteur, and PRACTIS for computer resources.

Supporting Information Available: Table of average interaction energies and fluctuations between the solute and the solvent in uranyl and strontium salts in IL solutions and eight figures. This material is available free of charge via the Internet at <http://pubs.acs.org>.

IC034281Y

(58) We notice the lack of experimental gas-phase data on, for example, $UO_2^{2+} \cdots S^-$ systems or on the interaction between the S^+ and S^- ionic components of ILs against which the QM computations could be compared. It should also be pointed out that polarization effects are magnified in $M^{n+} \cdots S$ dimers, as compared to condensed phases where the first coordination shell of the cation is saturated.

(59) Car, R.; Parrinello, M. *Phys. Rev. Lett.* **1985**, *55*, 2471–2474.

(60) Chipot, C. *J. Comput. Chem.* **2003**, *24*, 409–415 and references therein.

(61) Fuller, J.; Carlin, R. T.; Long, H. C. D.; Haworth, D. *J. Chem. Soc., Chem. Commun.* **1994**, 299–300.

(62) This can be seen from gas-phase simulations on $UO_2^{2+}(PF_6^-)_n$ clusters ($n = 6$ or 12) extracted from the last set of the dynamics in the [BMI][PF₆] solution (i.e., with 6 anions coordinated to UO_2^{2+} , as described in section 1, as described in section 1, plus six more remote anions (when $n = 12$)). Upon simulations of 1 ns at 200 K or 300 K, 2 PF_6^- ($n = 6$) or 8 PF_6^- ($n = 12$) anions dissociated, leading to an equatorial coordination of four anions only (two monodentate and two bidentate). The resulting CN is 6, which is larger than the CN of 5 in the $UO_2F_4(OH_2)^{2-}$ complex.^{63,64} The first-shell anions are quasi-static in the gas phase, which contrasts with the rapid spinning motions observed in IL solutions, “catalyzed” by neighboring imidazolium⁺ ions.

(63) Dao, N. Q. *Acta Crystallogr.* **1972**, *28B*, 2011–2015.

(64) Vallet, V.; Wahlgren, U.; Schimmelpennig, B.; Moll, H.; Szabo, Z.; Grenthe, I. *Inorg. Chem.* **2001**, *40*, 3516–3525.

(65) Jorgensen, W. L. *Acc. Chem. Res.* **1989**, *22*, 184–189.

(66) Hitchcock, P. B.; Mohammed, T. J.; Seddon, K. R.; Zora, J. A.; Hussey, C. L.; Ward, E. H. *Inorg. Chim. Acta* **1986**, *113*, L25–L26.

(67) Visser, A. E.; Jensen, M. P.; Laszak, I.; Nash, K. L.; Choppin, G.; Rogers, R. D. *Inorg. Chem.* **2003**, *42*, 2197–2199.